Journal of Magnetism and Magnetic Materials 540 (2021) 168454

Contents lists available at ScienceDirect

Journal of Magnetism and Magnetic Materials

journal homepage: www.elsevier.com/locate/jmmm

Research articles

Exploring the anti-site disorder and oxygen vacancies in Sr_2FeMoO_6 thin films

M. Saloaro [a], M.O. Liedke [b], I. Angervo [a], M. Butterling [b], E. Hirschmann [b], A. Wagner [b], H. Huhtinen [a,*], P. Paturi [a]

[a] Wihuri Physical Laboratory, Department of Physics and Astronomy, University of Turku, FI-20014 Turku, Finland
[b] Institute of Radiation Physics, Helmholtz-Zentrum Dresden - Rossendorf, Bautzner Landstraße 400, 01328 Dresden, Germany

ARTICLE INFO

Keywords:
Spintronics
SFMO
Defect engineering
Oxygen vacancy
Anti-site disorder
Positron annihilation spectroscopy
Magnetic properties

ABSTRACT

To address the importance of nanoscale defects in complex magnetic oxides, we present an effective tool, variable energy positron annihilation spectroscopy, for probing the relatively small changes in anti-site disorder and oxygen vacancies of the *in situ* annealed double perovskite Sr_2FeMoO_6 thin films. By controlling the annealing conditions in wide pressure and temperature ranges and thus affecting the amount of nanoscale defects, we show that the magnetic properties of Sr_2FeMoO_6 thin films can be modified, particularly with the oxygen nonstoichiometry, and hence their spintronic functionality can be improved. On the basis of our findings together with proposed mechanism, we suggest that the annealing treatments can also be scaled to other complex magnetic perovskites to engineer nanoscale defects and thus improve their usability in future spintronic applications.

1. Introduction

High quality thin films of multifunctional materials are needed for the novel spintronics and magnetoresistive applications. In particular, materials with the desired properties at room temperature (RT) are attractive for multilayer devices. Therefore, an outstanding candidate is $A_2BB'O_6$ type rock salt ordered double perovskite Sr_2FeMoO_6 (SFMO) (Fig. 1(a)), for which the Curie temperature (T_C) is clearly above room temperature, around 450 K [1]. In addition, SFMO possesses a large intrinsic magnetoresistance and as a half metallic material, 100 % spinpolarized charge carriers. However, the fabrication of SFMO thin films without deteriorating the magnetic and electrical properties is challenging and often results in lower T_C values compared with the polycrystalline bulk samples. Previous investigations have proposed that the nanoscale defects such as vacancies and anti-site disorder, where the B- and B'-site atoms swap their places, are the key factors in the optimization of the SFMO films towards applications [2–6]. In our recent study, the individual and collective role of substrate induced strain, oxygen vacancies (V_O) and anti-site disorder (ASD) were clarified with experimental data and theoretical analysis [7]. Our results showed the importance of the defect engineering, but no controlled route, to engineer these defects, was introduced. Since, it is commonly known that an experimental observation of V_O is challenging, the amount of oxygen vacancies was also indirectly observed in our previous work by comparing experimental and theoretical results. With this current investigation, we will make the next step and introduce a route to engineer nanoscale defects in SFMO thin films as well as a way to experimentally observe changes in the amount of oxygen vacancies in SFMO films.

In order to bring the high potential of SFMO for RT application into reality, the focus needs to be on T_C of the SFMO thin films without forgetting other magnetic properties such as spin polarization and saturation magnetization, M_s. Theoretical calculations as well as experimental studies for polycrystalline bulk SFMO have reported T_C values around 420–450 K [1,3,7–9]. Unfortunately, the Curie temperatures of SFMO thin films have not reached as high values and they have mostly been around 350 K [7,10,11], but higher values have also been reported [5,12]. However the determination of T_C is not explicit and both onset values and values determined as the minimum of the temperature derivative have been used, which may have a difference of several tens of degrees. Since the structural defects have been identified as crucial factors in improving the T_C of SFMO films, the results reported so far about their effect should also be considered. The past literature shows good consistency regarding the effect of ASD on the magnetic properties of SFMO. It has been reported that both the saturation magnetization and the Curie temperature decrease with increasing amount of ASD, which is also in good agreement with our recent results [2–4,7,13–15]. The results about the effect of oxygen vacancies are more limited and partly inconsistent. Fairly strong evidence about the decrease of M_s due to the increasing number of V_O has been provided [2,3,7,16–18]. However, one experimental study has suggested a decrease in T_C

* Corresponding author.
E-mail address: hannu.huhtinen@utu.fi (H. Huhtinen).

https://doi.org/10.1016/j.jmmm.2021.168454
Received 13 April 2021; Received in revised form 17 August 2021; Accepted 21 August 2021
Available online 28 August 2021

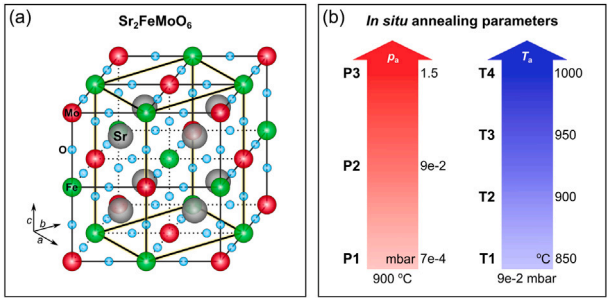

Fig. 1. (a) A schematic picture of the SFMO crystal lattice. (b) Illustration of the *in situ* annealing parameters of two SFMO sample series. The annealing pressure, p_a, (red arrow) and the annealing temperature, T_a, (blue arrow) increase from bottom to top. The P2/T2 sample is annealed at pressure and temperature used during the film deposition.

with the increasing number of V_O, while a theoretical study showed an opposite tendency [18]. Our recent experimental results support the theoretical study and show an increase in T_C with the increasing number of V_O [7].

Even though the effect of ASD and V_O on the magnetic properties of SFMO is fairly well known, no systematic way to control their amount in SFMO films has been proposed. In addition, according to our knowledge, no reports about experimental methods that can directly observe the amount of oxygen vacancies or changes in their amount in SFMO thin films have been shown. In this work, SFMO thin films, which were *in situ* annealed in three different annealing pressures, p_a, from 7×10^{-4} mbar to 1.5 mbar and at four different annealing temperatures from 850 °C to 1000 °C (Fig. 1(b) and Supplementary Material (SM)), were investigated. As a result, a route to engineer nanoscale defects in SFMO thin films by *in situ* annealing is presented and changes in the structural and magnetic properties induced by different annealing parameters are compared. The present report also shows that even the relatively small changes in the amount of V_O in SFMO thin films can be observed with positron annihilation spectroscopy (PAS).

2. Experimental details

The films were fabricated from a solid state target on $SrTiO_3$ (STO) (001) single crystal substrates using pulsed laser deposition (PLD). The deposition was made in the Ar atmosphere of 9 Pa with 2000 pulses at the substrate temperature of 900 °C. According to the results of our previous transmission electron microscopy measurements and the extrapolation of the X-ray reflectivity results, the pulse number of 2000 corresponds to the film thickness of around 160 nm [7,19]. Details of the film deposition and target preparation have been published earlier [11,20]. Films were *in situ* annealed in three different annealing pressures, p_a, from 7×10^{-4} mbar to 1.5 mbar and at four different annealing temperatures from 850 °C to 1000 °C as shown in Fig. 1(b) and in Table SI.

The XRD studies were made at room temperature with a Philips X'pert Pro MPD diffractometer. The measurements were carried out in the Bragg–Brentano θ - 2θ configuration using Cu K_α radiation, the Schulz texture goniometer and a PIXcel detector. Variable energy positron annihilation spectroscopy studies were performed at room temperature at the Apparatus for In-situ Defect Analysis (AIDA) [21] located at the Slow-Positron System of Rossendorf (SPONSOR) beamline [22], which provides mono-energetic and a magnetically guided variable energy positron beam. Positrons have been extracted from an intense ^{22}Na source and subsequently accelerated to discrete energy values in the range of 0.05–35 keV, which corresponds to depth sensitivity in the range of the surface region to about 4 μm for SFMO. Two characteristic methods have been utilized: (i) coincident Doppler broadening (cDB) of the annihilation line at fixed energy (3.85 keV) using two

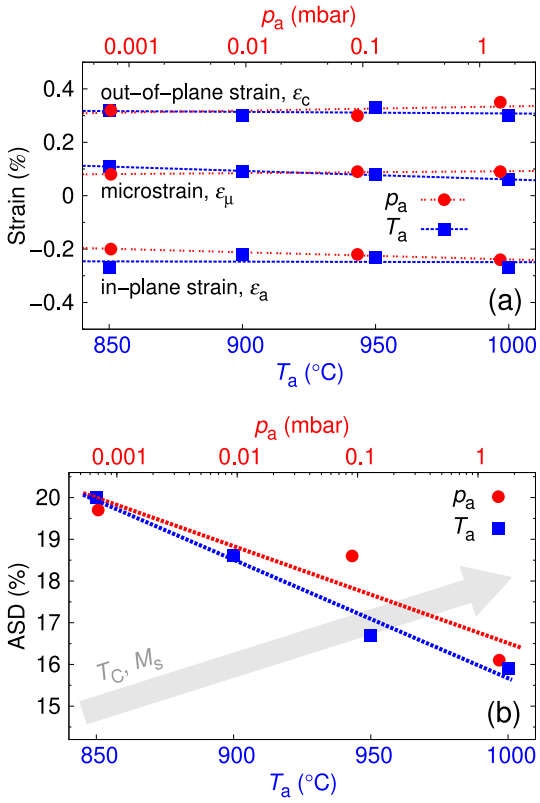

Fig. 2. In-plane and out-of-plane strains with the local microstrain values (a) and the amount of ASD (b) as a function of annealing pressure, p_a, (P1–P3 films) and temperature, T_a, (T1–T4 films). The correlation between decreasing amount of ASD and improved magnetic properties of SFMO thin films (T_C and M_s) from our earlier study [7] is presented with the grey arrow in (b).

High-Purity Germanium (HPGe) detectors with energy resolution of (780 ± 20) eV at 511 keV and (ii) standard single HPGe detector Doppler broadening (sDB) with an energy resolution of (1.09 ± 0.01) keV for the positron implantation energy scans, i.e. depth profiles.

Magnetic measurements were made with a Quantum Design MPMS SQUID magnetometer. The external magnetic field was parallel to the film plane during the measurements. The zero-field-cooled (ZFC) and field-cooled (FC) magnetization curves were measured in 100 mT and 500 mT fields. The Curie temperature was determined as a minimum of the temperature derivative of the 100 mT FC-curve. The hysteresis loops between −0.5 T and 0.5 T were measured at 10 K and 400 K. The dia- and paramagnetic signals from the substrate and the sample holder were subtracted from the measured data.

3. Results and discussion

3.1. The effect of *in situ* annealing on strain and anti-site disorder

The basic structural characterization of the films was made with X-ray diffraction (XRD). Details of these investigations are given in SM. The XRD measurements were also used in more sophisticated structural analysis, from which the substrate induced strains, full width at half maxima in ϕ (ϕ-FWHM) of the (204) peak and the amount of anti-site disorder (ASD) were obtained by the methods used before and explained in detail in Refs. [7,19]. As seen in Fig. 2(a), both the in-plane, ε_a, and the out-of-plane, ε_c, strains are independent of the *in situ* annealing treatments at various ambient Ar pressures and temperatures. The compressive in-plane strain, around −0.24 %, and the tensile out-of-plane strain, around 0.32 %, observed for the SFMO films on STO substrate are as expected of the compressive lattice mismatch

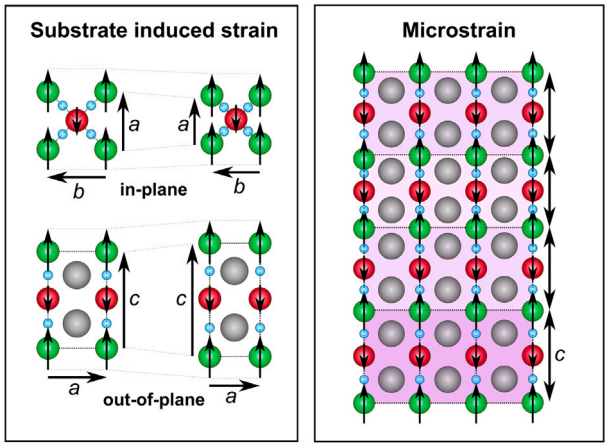

Fig. 3. A schematic illustration of the changes in in-plane and out-of-plane lattice parameters due to the substrate induced compressive strain (on the left) and variation of the c parameter observed as a microstrain, ϵ_μ (on the right), where darker background colour indicates the lengthened unit cell along the SFMO c axis.

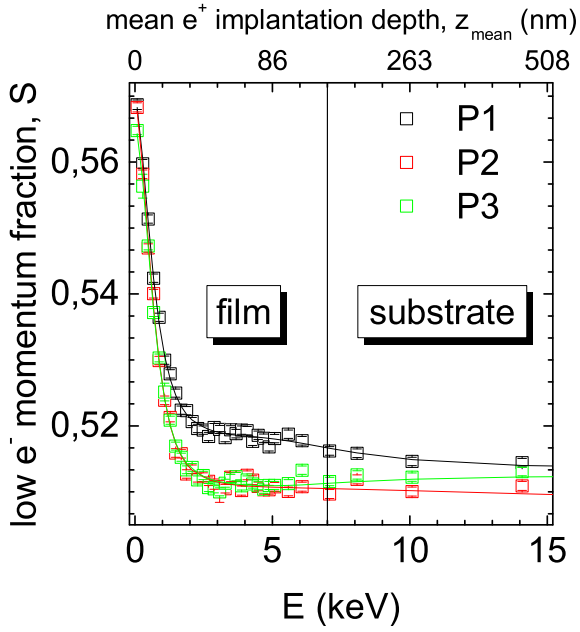

Fig. 4. Low momentum fraction S as a function of positron implantation energy, E and mean positron implantation depth, z_{mean}. The samples have been fabricated at three different Ar partial pressure conditions. Reduced Ar atmosphere induces oxygen vacancies, which are evidenced by increased S-parameter. Solid lines represent fits with the VEPFIT code [25]. The error bars are mostly within the square symbols.

and from our previous results [7,19,23]. As summarized in Fig. 3, substrate induced compressive strain from STO shortens the in-plane lattice parameters and elongates the out-of-plane lattice parameter of SFMO.

The microstrain, ϵ_μ, determined from the 2θ-FWHM of $(00l)$ peaks with the Williamson–Hall method (Fig. 2(a)) does not show notable annealing pressure, p_a, or annealing temperature, T_a, dependence either [24]. This means that the variation of the c parameter throughout the film thickness (see the rightmost picture of Fig. 3) does not change between the samples and is independent of the *in situ* annealing treatments. Similarly, the ϕ-FWHM is almost constant, around $(0.25 \pm 0.04)°$, in all the films. This indicates that the variations the in-plane crystal orientations due to the low angle grain boundaries exist in small amounts, but do not depend on the p_a or T_a. All in all, the films contain some amount of defects, such as the low angle grain boundary related stacking faults, which are typical in films grown on a substrate with lattice mismatch. This defect concentration has found to be lower in SFMO films grown on a substrate with relatively small lattice mismatch [19]. Since the lattice mismatch with the STO substrate used here is small and no changes in the microstrain or ϕ-FWHM with p_a or T_a were observed, these defects do not explain the possible changes between these films.

Unlike strains and the ϕ-FWHM, the amount of ASD shows clear dependence on the *in situ* annealing parameters (Fig. 2(b)). The amount of ASD decreases with increasing annealing pressure and annealing temperature. According to our earlier results, the decreasing amount of ASD increases T_C and M_s of SFMO films [7]. Therefore, the T_C and M_s of the films should increase with the increasing p_a and T_a as illustrated with the grey arrow in Fig. 2(b). However, our results about the magnetic properties cannot only be explained by the changing amount of ASD. This inconsistency is fully discussed in the following paragraphs.

3.2. The role of oxygen vacancies

In order to investigate the effect of *in situ* annealing on the amount of oxygen vacancies in our films, variable energy positron annihilation spectroscopy (VEPAS) measurements were carried out. Details of the measurement method are given in SM. In Fig. 4, the Doppler broadening of the annihilation line for a fraction of positrons annihilating with low momentum electrons (S-parameter) is presented as a function of positron implantation energy, E, for three different Ar partial pressures utilized during film deposition. The sample P1, annealed at the lowest Ar partial pressure, exhibits a clear increase in the S-parameter across the overall film thickness (see the top x-axis of Fig. 4), whereas samples P2 and P3, annealed at higher Ar partial pressures show both similar to each other but lower S value when compared with the P1. The increase of S-parameter originates from a formation of oxygen vacancies (V_O) in oxygen reduced atmosphere, which has been clearly evidenced by a number of positron annihilation spectroscopy (PAS) studies on perovskite materials, where vacuum annealing [26,27] and ion irradiation [28,29] has been used as a redox factor.

In general, oxygen vacancies are considered as donor-type defects because of the positive charge state. Positively charged vacancies are repulsive to positrons, however, transition-metal oxides have empty d orbitals that often can accommodate excess electronic charge, which turns V_O into a neutral charge state as long as the Fermi level is located on the upper side in the band gap [30]. Keeble et al. [31] has calculated positron lifetimes for complex perovskites like $SrTiO_3$ and $Sr_3Ru_2O_7$ and found only small variations of lifetimes representing A- and B-site vacancies in ABO_3 systems. DFT calculations of SFMO [18] are more complex and were not performed for this data, but positron lifetimes are expected to be in the similar range regarding a large difference for A- and B-site defects. For materials like STO, the partial occupation of the conduction band occurs due to the introduction of V_O as a consequence of the electron transfer into the Ti $3d$ band, i.e., electrons enter Ti $3d$ states due to lack of O $2p$ states. Thus, the charge of oxygen vacancies and their related defects is locally compensated by the charge transfer to Ti [26]. In addition, defect complexes, such as a V_{Sr}-V_O pairs are known to trap positrons due to their neutral or even negative charge state [27]. Existence of such complexes in our SFMO films is reflected by increased S-parameter (Fig. 4) and coincidence Doppler broadening results (see Fig. 5).

The positron effective diffusion length, L_+, was about 4 nm for the films P2 and P3 and substrate, which suggests large defect concentration overall. For the P1 sample, L_+ is larger about 5.5 nm and 36 nm, respectively. Although slightly larger positron diffusion length, L_+, for the P1 sample appears to be contradicting with increased S, it could, however, originate from (i) re-oxidized surface region with lower vacancy concentration and/or (ii) the existence of the electrical

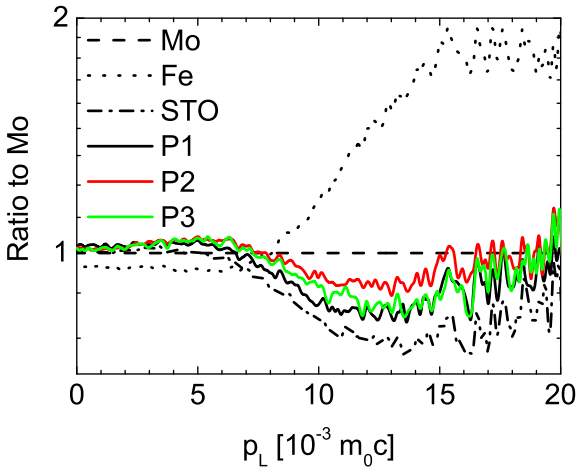

Fig. 5. Coincidence Doppler broadening spectra normalized to a Mo reference sample, measured at $E = 3.85$ keV, which corresponds approximately to the middle of the film. The electronic structure of all the systems deposited at different Ar pressure conditions resembles well annealed STO sample.

field due to a difference in conductance between surface and interface regions. Nevertheless, the S-parameter is strongly increased for the P1 sample, which is the absolute measure of defect concentration and/or defect size, whereas L_+ is an effective contribution from certain sample regions only. The more detailed discussion on this issue can be found in the SM.

In Fig. 5, ratio plots normalized to Mo reference sample resulting from coincidence Doppler broadening measurements are presented. A comparison to STO annealed in the vacuum at 1000 °C and defect free Fe reference samples is also given. It is clear that electronic structure of a defect site where positrons are localized is very similar to the STO reference sample. At the same time, its atomic surrounding shows enlarged Mo occupation, whereas Fe is mostly not represented at the high momentum part for $p_L > 8 \cdot 10^{-3}$ m_0c. The sample P2 exhibits the largest number of Mo nearest-neighbours around the defect among all the samples. We have suggested that positrons in our STO reference sample should mostly localize in Ti vacancies, however, here Ti atoms are absent but still all the ratio plots for SFMO samples have very similar shape as the STO reference sample, thus exhibiting very similar electronic structure. This finding suggests that the dominant types of defects in SFMO films consist of Sr vacancies (and V_{Sr}-V_O complexes), which are the second common type of vacancies after V_{Ti} in STO. This is strongly supported by additional cDB measurements on the same samples performed six months later, where the electronic structure has changed even more to resemble the STO reference due to samples ageing and V_O re-oxidation (see SM Fig. S5). Not only the electronic structure has changed, but likely the defect types within the film and the substrate as well, where a clear decrease of the S-parameter is found, which suggests a decrease of V_O concentration (see SM Fig. S4). It is likely that annealing in oxygen refills larger complexes and generates the simpler B-site + V_O complex instead, but generally reducing concentration of oxygen vacancies [32,33].

3.3. Influence on magnetic properties

Our previous results, which are in good agreement with the theoretical results of M. Hoffmann et al. [18], have shown that the increasing amount of oxygen vacancies actually increases the T_C of SFMO while the M_s decreases [7,18]. As mentioned before, these results also indicate that increasing the amount of ASD decreases both T_C and M_s [7]. In order to complete the whole picture of the effects that *in situ* annealing has on the SFMO films, the magnetic properties were also investigated. The magnetic properties were determined from

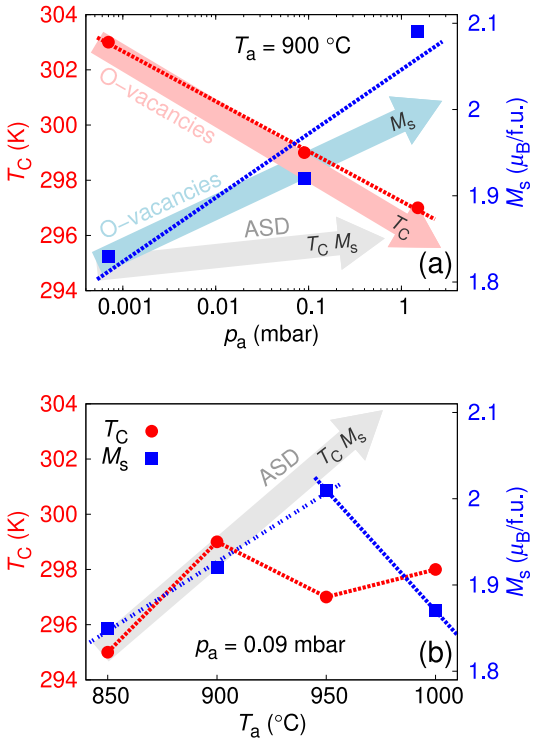

Fig. 6. The annealing pressure (a) and temperature (b) dependence of Curie temperature (red dots) and saturation magnetization (blue squares) for SFMO thin films. The grey arrows represent the effect of decreasing the amount of ASD on the T_C and M_s. Similarly, the red and blue arrows represent the effect of decreasing the amount of V_O on the T_C and M_s according to our earlier study [7]. The amount of ASD and oxygen vacancies decreases from left to right.

the measured $M(T)$- and $M(B)$-curves, which are shown together with the details of the magnetic investigations in the SM. Aside from the clear minimum from which the T_C was obtained, some of the dM/dT-curves also show traces of an additional SFMO phase with higher T_C (see SM). The additional SFMO phase seems to be related to the T_a and it appears when the annealing temperature exceeds 850 °C. Since the *in situ* annealing is made after deposition, it is possible that the top layers of the film are more affected by the heat treatment than the bottom layers, which results in two slightly different SFMO phases within one film.

The Curie temperature values together with the saturation magnetization obtained from the 10 K hysteresis loops are presented as a function of *in situ* annealing parameters in Fig. 6. In both film series, a decrease in the amount of ASD with increasing annealing temperature and pressure was observed. Based on our earlier results, this would mean an increase in T_C and M_s with increasing p_a and T_a as represented with the grey arrow in Fig. 6. The annealing temperature series follows this finding quite well in the low T_a part (Fig. 6(b)). The M_s increases with increasing T_a until 950 °C is reached, at which point the dependence turns into a decreasing one. The Curie temperature also shows a slightly increasing trend between 850 °C and 900 °C above which the T_C remains approximately constant. The annealing at higher temperatures could lead to interdiffusion at the film/substrate interface, which would cause changes in the magnetic properties of the films. However, in approximately 160 nm thick films, the effect of interdiffusion is very small and based on our previous results, no notable interdiffusion has occurred at the SFMO/STO interface [19]. Therefore, it cannot explain these results. Instead, the sudden decrease of M_s suggests that additional oxygen vacancies are introduced to the film when annealed at 1000 °C. This should also lead to an increase in T_C, which was not observed. However, traces of two SFMO phases

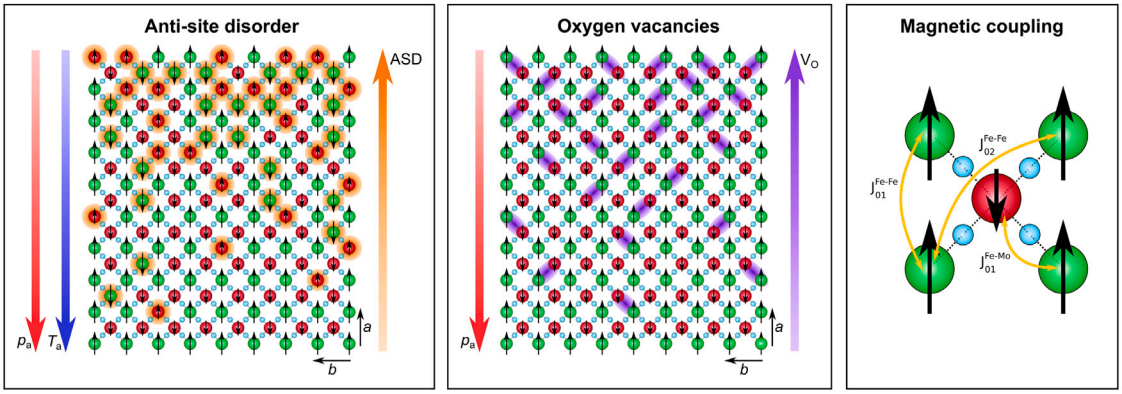

Fig. 7. A schematic picture of the effect of annealing conditions on the amount of anti-site disorder and oxygen vacancies (first two from the left). The annealing pressure increases along the red arrows and the annealing temperature along the blue arrow. The number of anti-site disorder and oxygen vacancies increases in the opposite direction than p_a and T_a. The rightmost picture illustrates the three most important magnetic coupling pairs between Fe–Fe and Fe–Mo [18]. Green circles represent Fe, red circles Mo and light blue circles O.

were observed in the dM/dT-curves of films *in situ* annealed at least at 900 °C, where indication of ≈ 20 K higher T_C can be seen, making it possible that the effect of annealing is stronger in surface layers of the film. Hence, it is possible that the surface of the films contains more oxygen vacancies than the part next to the substrate interface. This would increase the T_C of the additional phase keeping the T_C of the dominating bottom phase unchanged, as observed. The higher oxygen vacancy concentration would also decrease the M_s of the surface layers leading to a decrease in the total M_s of the film as observed in films with T_a high enough.

The annealing pressure dependence of T_C and M_s cannot only be explained with ASD either and it seems that the oxygen vacancies play a greater role in these films. Our PAS results suggested a larger number of V_O in the film annealed at low pressure, which is supported by increased T_C and decreased M_s observed in this film (Fig. 6(a)). Overall, the T_C seems to decrease and M_s increase with increasing annealing pressure, which could be explained by the combined effect of decreasing number of ASD and oxygen vacancies. The arrows in Fig. 6(a) illustrate their individual effects on the magnetic properties of SFMO films, which in combination leads to the observed trends in T_C and M_s. However, our PAS results indicate the possibility of Sr vacancies in our films, which is also supported by our earlier theoretical results [34]. The effect of V_{Sr} is not yet well known and needs to be investigated in more detailed in the future, but L. Harnagea and P. Berthet have suggested a decrease in T_C and M_s in Sr-deficient SFMO samples [6].

To summarize, we have combined the mechanisms behind the formation of the nanoscale defects in a schematic illustration of Fig. 7. First of all, the structural and magnetic properties suggest that we have been able to affect the number of ASD and oxygen vacancies in SFMO thin films by *in situ* annealing. Decreasing the annealing pressure and annealing temperature both show a slight increasing effect on the amount of ASD, which leads to a decreased T_C and M_s. Due to the ASD, the Fe ions in the Mo site are strongly antiferromagnetically coupled to other Fe ions, which reduces M_s and T_C until higher ASD concentrations are reached [7]. The influence of the treatment is much more prominent for oxygen stoichiometry, since the increased amount of oxygen vacancies due to *in situ* annealing at low pressure increases the T_C and decreases M_s of SFMO. According to M. Hoffmann et al. this behaviour can be understood by the magnetic exchange interactions up to the next nearest neighbour Fe ions (Fig. 7) [18]. Oxygen vacancies reduce the exchange between Fe ions (J_{01}^{Fe--Fe} and J_{02}^{Fe--Fe}) and favour the exchange between Fe and Mo ions (J_{01}^{Fe--Mo}), which together leads to reduced total magnetic moment and smaller M_s. On the other hand, the antiferromagnetic coupling between Fe and Mo is stronger and mediates additional ferromagnetic coupling, which results in increased Curie temperature.

4. Conclusions

Our results show that anti-site disorder and oxygen vacancies can be controlled in SFMO thin films by *in situ* annealing treatments. By decreasing the annealing pressure, we were able to increase the amount of both ASD and V_O, and these together lead to an increased T_C and reduced M_s. The increasing amount of V_O alone has the same increasing effect on T_C as these two together, but the increasing amount of ASD alone leads to decreased T_C. This suggests that the effect of oxygen vacancies on the magnetic properties is more dominant than the effect of ASD. Similarly, the decreasing annealing temperature induced less ASD in SFMO thin films, but the magnetic behaviour in the high annealing temperature range suggested the additional defects or inhomogeneous effect of the annealing through film thickness, which needs to be investigated in more detail in the future. The role of defect engineering is important and the nanoscale defects such as ASD and V_O are key factors also in other perovskite materials. In addition, the positron annihilation spectroscopy turned out to be an excellent tool for exploring the nanoscale defects through the whole film and, by using the *in situ* annealing treatments, we were able to study the sensitivity of the method and detect the threshold limits to observe the minor amount of anti-site disorder and oxygen vacancies.

Declaration of competing interest

The authors declare that they have no known competing financial interests or personal relationships that could have appeared to influence the work reported in this paper.

Acknowledgement

The Jenny and Antti Wihuri Foundation, Finland is acknowledged for financial support.

Appendix A. Supplementary data

Supplementary material related to this article can be found online at https://doi.org/10.1016/j.jmmm.2021.168454.

References

[1] K.-I. Kobayashi, T. Kimura, H. Sawada, K. Terakura, Y. Tokura, Nature 395 (677) (1998).
[2] S. Colis, D. Stoeffler, C. Meny, T. Fix, C. Leuvrey, G. Pourroy, A. Dinia, P. Panissod, J. Appl. Phys. 98 (2005) 033905.
[3] A.S. Ogale, S.B. Ogale, R. Ramesh, T. Venkatesan, Appl. Phys. Lett. 75 (537) (1999).

[4] D. Sánchez, M. García-Hernández, N. Auth, G. Jakob, J. Appl. Phys. 96 (2736) (2004).
[5] A.J. Hauser, R.E.A. Williams, R.A. Ricciardo, A. Genc, M. Dixit, J.M. Lucy, P.M. Woodwart, H.L. Fraser, F. Yang, Phys. Rev. B 83 (2011) 014407.
[6] L. Harnagea, P. Berthet, J. Solid State Chem. 222 (115) (2015).
[7] M. Saloaro, M. Hoffmann, W.A. Adeagbo, S. Granroth, H. Deniz, H. Palonen, H. Huhtinen, S. Majumdar, P. Laukkanen, W. Hergert, A. Ernst, P. Paturi, ACS Appl. Mater. Interfaces 8 (20440) (2016).
[8] J. Raittila, T. Salminen, T. Suominen, K. Schlesier, P. Paturi, J. Phys. Chem. Solids 67 (1712) (2006).
[9] T. Suominen, J. Raittila, T. Salminen, K. Schlesier, J. Linden, P. Paturi, J. Magn. Magn. Mater. 309 (278) (2007).
[10] D. Sanchez, N. Auth, G. Jakob, J.L. Martinez, M. Garcia-Hernandes, J. Magn. Magn. Mater. 294 (2005) e119.
[11] P. Paturi, M. Metsänoja, H. Huhtinen, Thin Solid Films 519 (8047) (2011).
[12] A. Venimadhav, F. Sher, J.P. Attfield, M.G. Blamire, J. Magn. Magn. Mater 269 (101) (2004).
[13] A. Venimadhav, M.E. Vickers, M.G. Blamire, Solid State Commun. 130 (631) (2004).
[14] B.J. Park, H. Han, J. Kim, Y.J. Kim, C.S. Kim, B.W. Lee, J. Magn. Magn. Mater. 272-276 (2004) 1851.
[15] Y. Moritomo, N. Shimamoto, S. Xu, A. Machida, E. Nishibori, M. Takata, M. Sakata, A. Nakamura, Jpn. J. Appl. Phys. 40 (672) (2001).
[16] R. Kircheisen, J. Töpfer, J. Solid State Chem. 185 (76) (2012).
[17] J. Töpfer, R. Kircheisen, S. Barth, J. Appl. Phys. 105 (07D712) (2009).
[18] M. Hoffmann, V.N. Antonov, L.V. Bekenov, K. Kokko, W. Hergert, A. Ernst, J. Phys.: Condens. Matter 30 (2018) 305801.
[19] M. Saloaro, H. Deniz, H. Huhtinen, H. Palonen, S. Majumdar, P. Paturi, J. Phys. Cond. Mat. 27 (2015) 386001:1–11.
[20] I. Angervo, M. Saloaro, J. Tikkanen, H. Huhtinen, P. Paturi, Appl. Surf. Sci. 396 (754) (2017).
[21] M.O. Liedke, W. Anwand, R. Bali, S. Cornelius, M. Butterling, T.T. Trinh, A. Wagner, S. Salamon, D. Walecki, A. Smekhova, H. Wende, K. Potzger, J. Appl. Phys. 117 (2015) 163908:1–6.
[22] W. Anwand, G. Brauer, M. Butterling, H.R. Kissener, A. Wagner, Defect Diffus. Forum 331 (2012) 25–40.
[23] I. Angervo, M. Saloaro, H. Huhtinen, P. Paturi, Appl. Surf. Sci. 422 (682) (2017).
[24] M. Birkholz, Thin Film Analysis By X-Ray Scattering, Wiley-VCH, 2006.
[25] A. van Veen, H. Schut, J. de Vries, R. Hakvoort, M. Ijpma, AIP Conf. Proc. 218 (171) (1990).
[26] A. Uedono, K. Shimayama, M. Kiyohara, Z.Q. Chen, K. Yamabe, J. Appl. Phys. 92 (2002) 2697–2702.
[27] A. Uedono, M. Kiyohara, N. Yasui, K. Yamabe, J. Appl. Phys. 97 (2005) 033508:1–5.
[28] A. Gentlis, O. Copie, G. Herranz, F. Fortuna, M. Bibes, K. Bouzehouane, É. Jacquet, C. Carrétéro, M. Basletić, E. Tafra, A. Hamzić, A. Barthélémy, Phys. Rev. B 81 (2010) 144109.
[29] G. Herranz, O. Copie, A. Gentlis, E. Tafra, M. Basletić, F. Fortuna, K. Bouzehouane, S. Fusil, É. Jacquet, C. Carrétéro, M. Bibes, A. Hamzić, A. Barthélémy, J. Appl. Phys. 107 (2010) 103704.
[30] S. Pöykkö, D.J. Chadi, Appl. Phys. Lett. 76 (499) (2000).
[31] D.J. Keeble, S. Wicklein, R. Dittmann, L. Ravelli, R.A. Mackie, W. Egger, Phys. Rev. Lett. 105 (2010) 226102.
[32] D.J. Keeble, R.A. Mackie, W. Egger, B. Löwe, P. Pikart, C. Hugenschmidt, T.J. Jackson, Phys. Rev. B 81 (2010) 064102.
[33] M. Qin, F. Gao, J. Cizek, S. Yang, X. Fan, L. Zhao, J. Xu, G. Dong, M. Reece, H. Yan, Acta Mater. 164 (2019) 77–89.
[34] W.A. Adeagbo, M. Hoffmann, A. Ernst, W. Hergert, M. Saloaro, P. Paturi, K. Kokko, Phys. Rev. Mater. 2 (2018) 083604.